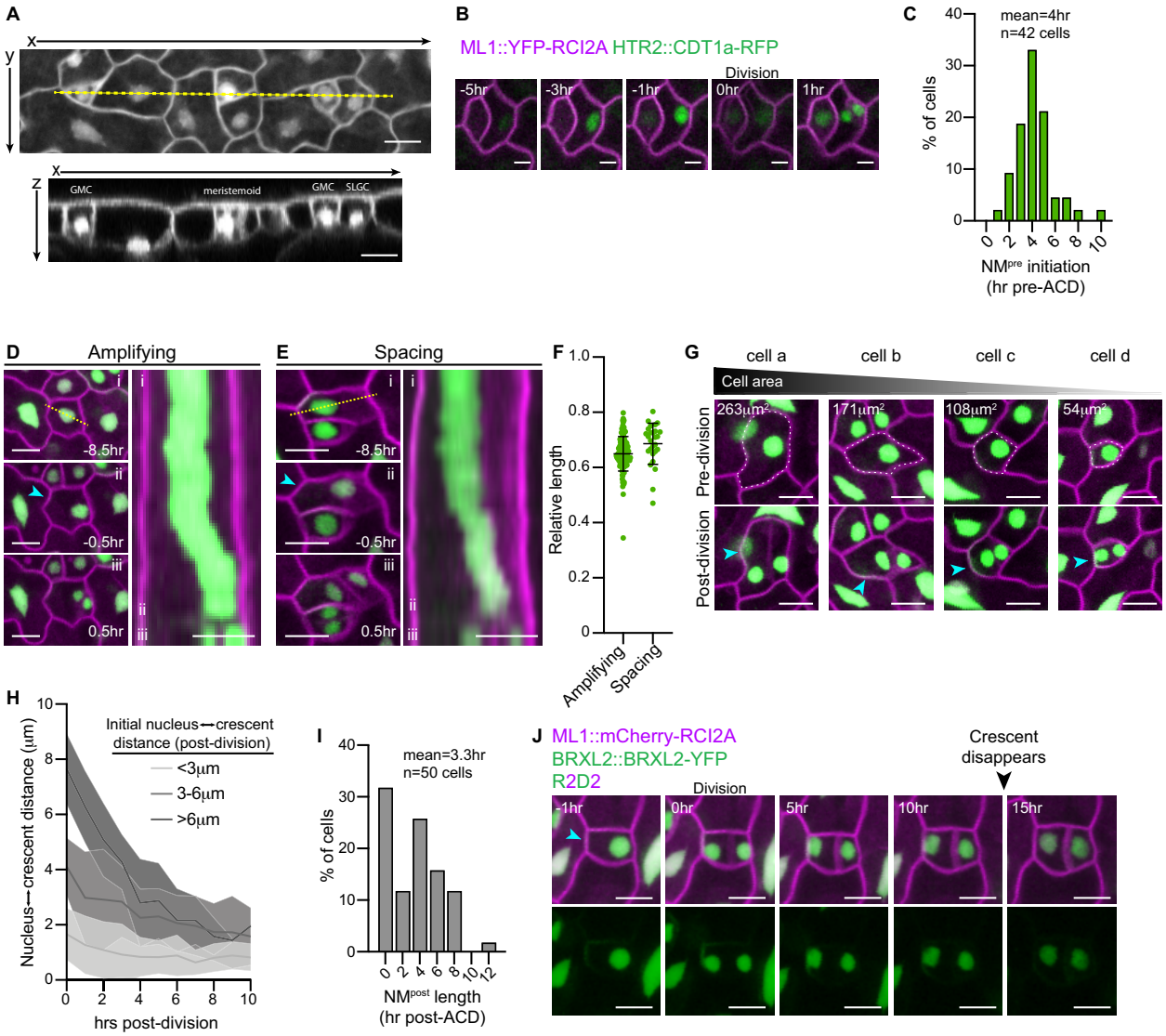

Figure S1. Characterization of NM^{pre} and NM^{post}. Related to Figure 1.

A. Top-down (top) and orthogonal (bottom, generated along the dotted yellow line) views of the leaf epidermis, stained with propidium iodide. Scale bars-10μm.

B. Stills from time-lapse imaging of the ML1::YFP-RCI2A HTR2::CDT1a-RFP line. Note that CDT1a expression becomes detectable shortly before NM^{pre} onset. Scale bars-5μm.

C. Timing of NM^{pre}, measured relative to hours before mitotic onset. n-42 cells.

D. Stills (left) and kymograph (right) of nuclear position during amplifying division. Stills of nuclear movement (i) 8.5hr before division, (ii) 0.5hr before division, and (iii) 0.5hr post-ACD (iii). Kymograph generated from dotted line shown in (i) (right). The cyan arrowhead indicates the polarity crescent. Scale bars-10μm.

E. Stills (left) and kymograph (right) of nuclear position during spacing division, formatted as in Figure S1E. The cyan arrowhead indicates the polarity crescent. Scale bars-10μm.

F. Nuclei are asymmetrically positioned in both amplifying and spacing divisions. Data are derived from the same cells as those used in Figure 1G and 1H. Amplifying-113 cells, spacing-27 cells. Data are represented as mean±standard deviation.

G. Four examples of morphologically varied progenitors with the indicated cell areas before and after ACD. The cyan arrowheads indicate the polarity crescents. Scale bars-10μm.

H. Average nucleus-to-crescent distance during NM^{post}, binned according to the initial nucleus-to-crescent distance. Data are derived from the same cells as those used in Figure 1L. <3μm-38 cells, 3-6μm-27 cells, >6μm-5 cells. Data are represented as mean± standard deviation.

I. Distribution of NM^{post} lengths.

J. Stills from time-lapse imaging showing nuclear capture by the polarity crescent. Note that the nucleus has moved away from the membrane at 15hr. The cyan arrowhead indicates the polarity crescent. Scale bars-10μm.

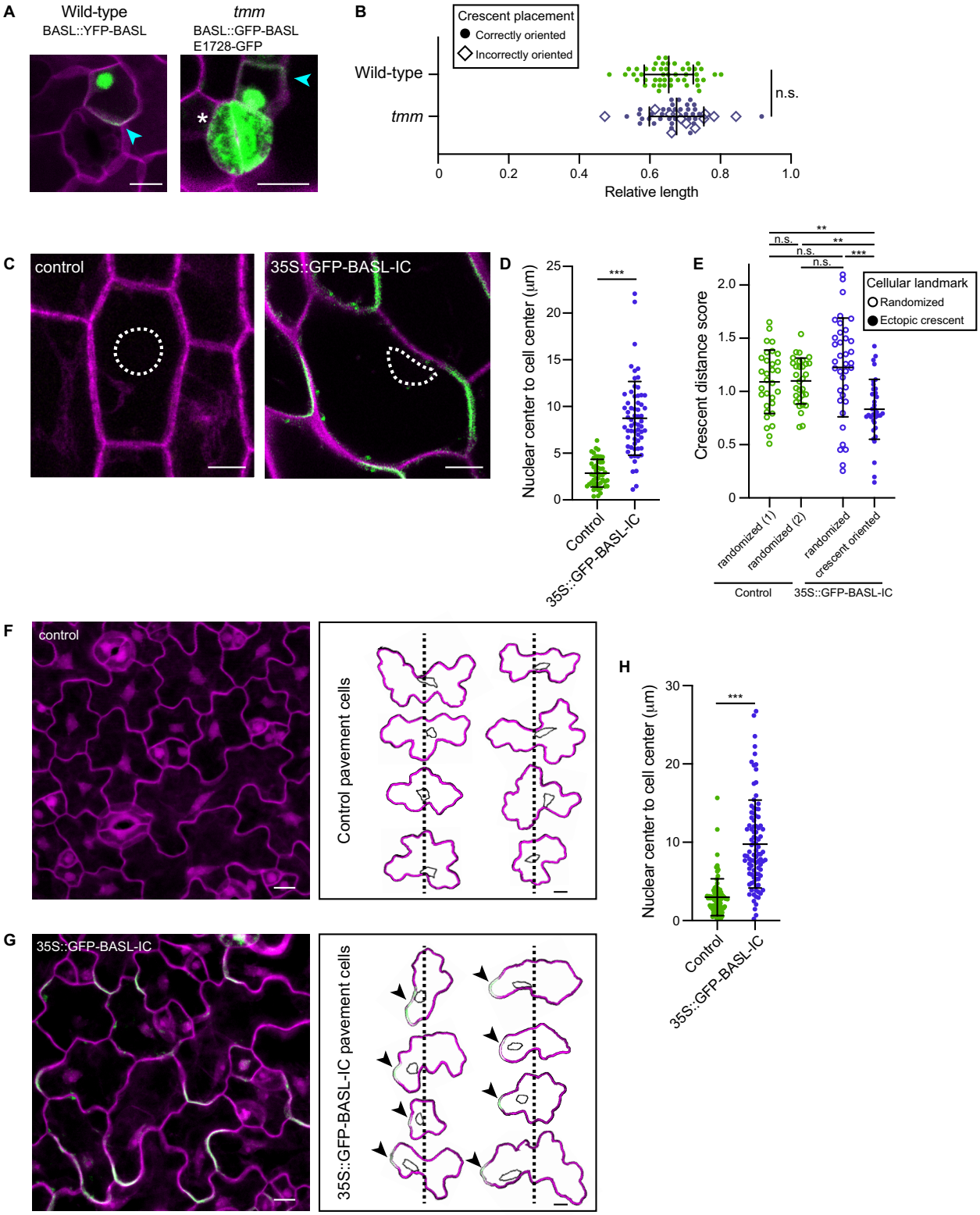
A
Wild-type
BASL::YFP-BASL
tmm
BASL::GFP-BASL
E1728-GFP
B
Crescent placement
Correctly oriented
Incorrectly oriented
Wild-type
tmm
n.s.
0
0.2
0.4
0.6
0.8
1.0
Relative length
C
control
35S::GFP-BASL-IC
D
Nuclear center to cell center (μm)
***
Control
35S::GFP-BASL-IC
E
Crescent distance score
n.s.
**
***
Cellular landmark
Randomized
Ectopic crescent
randomized (1)
randomized (2)
randomized
crescent oriented
Control
35S::GFP-BASL-IC
F
control
Control pavement cells
G
35S::GFP-BASL-IC
35S::GFP-BASL-IC pavement cells
H
Nuclear center to cell center (μm)
***
Control
35S::GFP-BASL-IC

Figure S2. BASL polarity controls nuclear position. Related to Figure 2.

A. Representative images of the pre-ACD nuclear position in wild-type (BASL::YFP-BASL ML1::mCherry-RCI2A) and *tmm* (*tmm* BASL::GFP-BASL E1728-GFP, stained with propidium iodide). Measurements were performed using BASL reporters, which are localized to the polarity crescent (cyan arrowheads) and the nuclei before division. Note * where the GFP expression in mature guard cells in *tmm* is due to E1728-GFP, an additional reporter in this genetic background. Scale bars-10μm.

B. Quantification of the pre-ACD nuclear position in wild-type and *tmm*. A subset of cells in *tmm* have obviously misplaced polarity crescents, indicated by the diamonds. Nuclear position in this population of *tmm* cells is not statistically distinct from the total *tmm* population. Wild-type-48 cells, *tmm*-46 cells. Data are represented as mean±standard deviation. n.s.-not significant.

C. Representative images of the nuclear position in hypocotyl epidermal cells in wild-type and 35S::GFP-BASL-IC-expressing plants, stained with propidium iodide (magenta). The dotted outline indicates the nuclear position. Scale bars-10μm.

D. Quantification of the distance from the nuclear center to the cell center in wild-type and 35S::GFP-BASL-IC-expressing hypocotyl epidermal cells. Wild-type-48 cells, 35S::GFP-BASL-IC-63 cells. Data are represented as mean±standard deviation. ***-$p<0.001$.

E. Quantification of the crescent distance score in wild-type and 35S::GFP-BASL IC-expressing hypocotyls. The crescent distance score reflects the ratio of the average distance of the nucleus to the crescent to the average distance of the nucleus to the rest of the cell cortex. A score <1 indicates that the nucleus is closer to the crescent than the rest of the cell cortex. Because control cells lack a crescent, the cells were randomly oriented, and a crescent-sized region of the membrane was chosen for the measurement. Randomized (1) and randomized (2) show the results of choosing different, opposing “crescent” regions on the same rotated control cells. Randomized 35S::GFP-BASL-IC measurements were generated by randomly orienting 35S::GFP-BASL-IC cells and choosing a crescent-sized region of the membrane, as for control cells. See the STAR Methods for additional information. Data are represented as mean± standard deviation. n.s.-not significant, *** - $p<0.001$.

F. Representative image (left) showing the nuclear positions in propidium iodide-stained wild-type pavement cells. (Right) Representative examples of segmented wild-type

pavement cells with black outlines indicating the nuclear positions; these cells were chosen from a field of view that extends beyond the borders of the cropped image on the left. The vertical dotted line is used to align the cell centers. Because pavement cells in wild-type cotyledons lack an intrinsic polarity orientation, the segmented cells were randomly oriented along their long axes. Scale bars-10μm.

G. Representative image (left) showing the nuclear positions in propidium iodide-stained 35S::GFP-BASL-IC-expressing pavement cells. (Right) Representative examples of segmented 35S::GFP-BASL-IC pavement cells with black outlines indicating the nuclear positions; these cells were chosen from a field of view that extends beyond the borders of the cropped image on the left.. The vertical dotted line is used to align the cell centers. All pavement cells were oriented with the ectopic polarity crescents to the left, indicated by the black arrows. Scale bars-10μm.

H. Quantification of the distance from the nuclear center to the cell center in wild-type and 35S::GFP-BASL-IC-expressing pavement cells. Wild-type-87 cells, 35S::GFP-BASL-IC-95 cells. Data are represented as mean±standard deviation. ***-$p<0.001$.

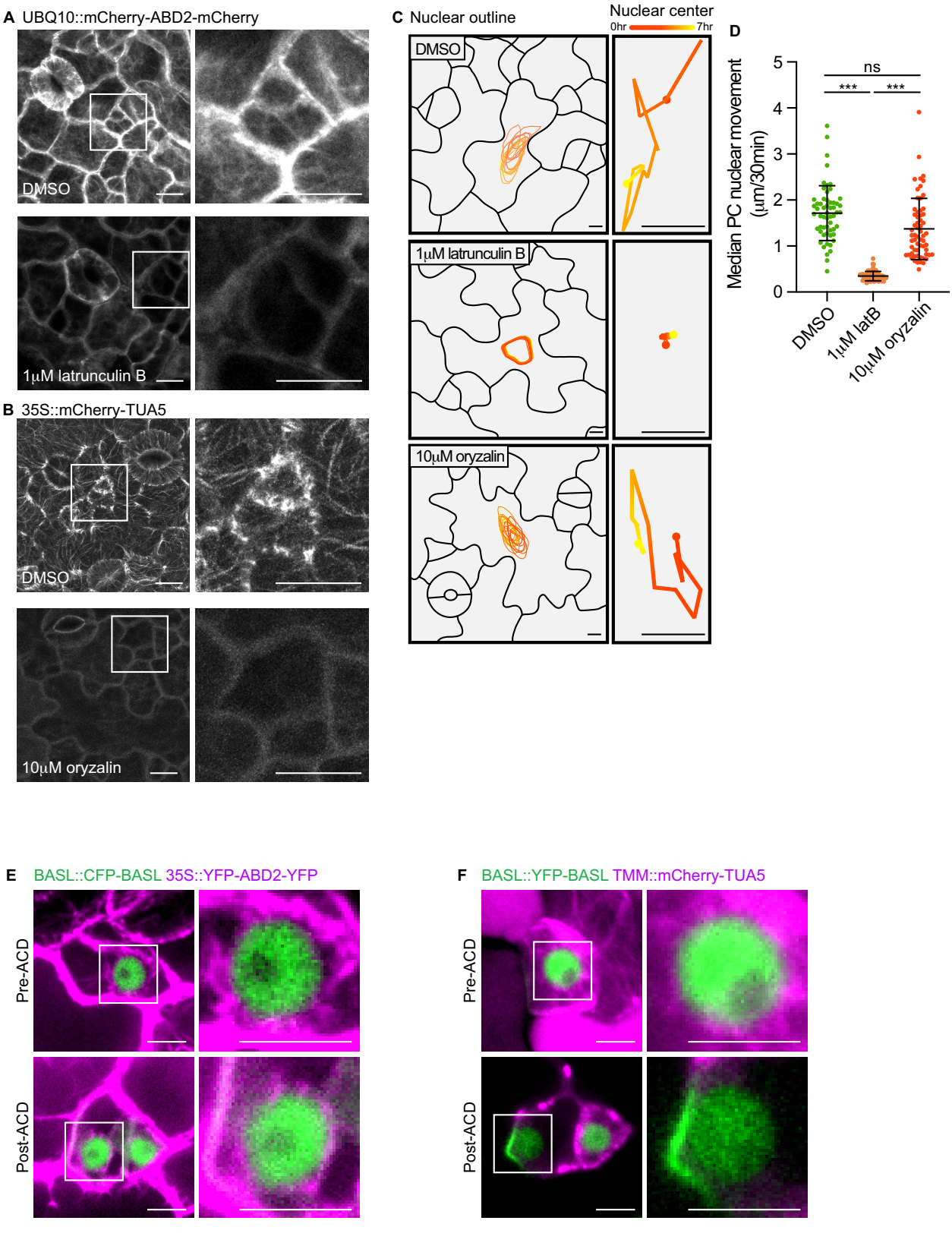
A UBQ10::mCherry-ABD2-mCherry
DMSO
1μM latrunculin B
B 35S::mCherry-TUA5
DMSO
10μM oryzalin
C Nuclear outline
Nuclear center
0hr
7hr
DMSO
1μM latrunculin B
10μM oryzalin
D
Median PC nuclear movement (μm/30min)
ns
***
***
DMSO
1μM latB
10μM oryzalin
E BASL::CFP-BASL 35S::YFP-ABD2-YFP
Pre-ACD
Post-ACD
F BASL::YFP-BASL TMM::mCherry-TUA5
Pre-ACD
Post-ACD

Figure S3. Controls for pharmacological perturbations of the cytoskeleton. Related to Figure 3.

A. Representative images of the cotyledon epidermis expressing the actin reporter UBQ10::mCherry-ABD2-mCherry upon DMSO (top) or 1μM latrunculin B (bottom) treatment. (Right) Zoomed regions are from the white boxes in the left images that highlight actin organization upon drug treatment in early stomatal lineage cells. Scale bars-10μm.
B. Representative images of the cotyledon epidermis expressing the microtubule reporter 35S::mCherry-TUA5 upon DMSO (top) or 10μM oryzalin (bottom) treatment. (Right) Zoomed regions are from the white boxes in the left images that highlight microtubule organization upon drug treatment in early stomatal lineage cells Scale bars-10μm.
C. Nuclear tracking in pavement cells over 7 hours (each outline represents the nuclear position at 30 minute intervals) (left). Tracking of the nuclear center upon the indicated treatments (right). Scale bars-5μm.
D. Quantification of pavement cell nuclear movement (median distance traveled every 30 min). Each point represents the median value for a single pavement cell. DMSO-57 cells, latB-64 cells, oryzalin-61 cells. Data are represented as mean±standard deviation. n.s.-not significant, *** - $p<0.001$.
E. F-actin association with the nucleus (BASL::CFP-BASL 35S::YFP-ABD2-YFP) before and after ACD. (Right) Zoomed regions are from the white boxes in the left images that highlight perinuclear actin association. Scale bars-5μm.
F. Microtubule association with the nucleus (BASL::YFP-BASL TMM::mCherry-TUA5) before and after ACD. Arrows indicate the position of the nuclei. (Right) Zoomed regions are from the white boxes in the left images that highlight perinuclear microtubule association. Scale bars-5μm.

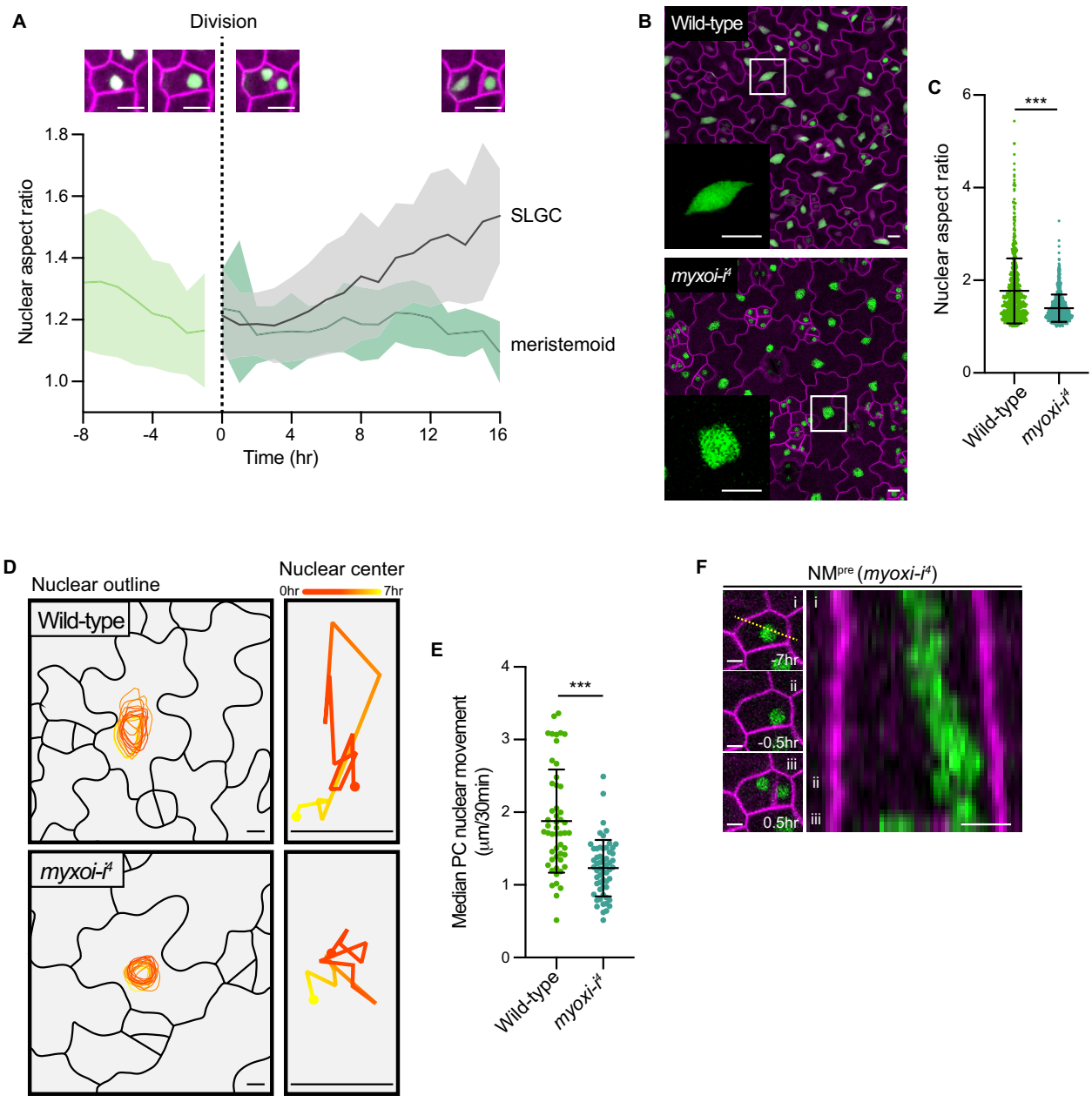

Figure S4. Additional characterization of *myoxi-i*^{4}. Related to Figure 4.

A. Nuclear aspect ratios during ACD. Pre-ACD-28 cells, SLGC-22 cells, meristemoid-29 cells. Images on the top show a representative cell undergoing ACD, highlighting the nuclear shape changes quantified in the graph. Scale bars-10μm. Data are represented as mean±standard deviation.

B. Representative images of nuclear shape in wild-type (R2D2 BRXL2::BRXL2-YFP ML1::mCherry-RCI2A) and *myoxi-i*^{4} (*myoxi-i*^{4} ML1::H2B-YFP ML1::mCherry-RCI2A) cotyledons. Scale bars-10μm.

C. Quantification of pavement cell nuclear aspect ratio. Wild-type-639 cells, *myoxi-i*^{4}-770 cells. Data are represented as mean±standard deviation. *** - $p<0.001$.

D. Nuclear tracking in wild-type and *myoxi-i*^{4} pavement cells over 7 hours (each outline represents the nuclear position at 30 minute intervals). Tracking of the nuclear center (right). Scale bars-5μm.

E. Quantification of median nuclear movement per 30 minutes in wild-type and *myoxi-i*^{4} pavement cells. WT-51 cells, *myoxi-i*^{4}-57 cells. Data are represented as mean±standard deviation. *** - $p<0.001$.

F. Stills (left) and kymograph (right) of NM^{pre} in *myoxi-i*^{4}. Stills correspond to the indicated time frames in the kymograph showing (i) 7hr pre-ACD, (ii) 0.5hr pre-ACD, (iii) 0.5hr post-division. Scale bars-5μm.